NIH Public Access
Author Manuscript
Neuron. Author manuscript; available in PMC 2010 November 25.

Published in final edited form as:
Neuron. 2009 November 25; 64(4): 471–483. doi:10.1016/j.neuron.2009.09.025.

Peptidyl-prolyl isomerase FKBP52 controls chemotropic guidance of neuronal growth cones via regulation of TRPC1 channel opening

Sangwoo Shim[1,2,*], **Joseph P. Yuan**[3,4,*], **Ju Young Kim**[1,2], **Weizhong Zeng**[4], **Guo Huang**[3], **Aleksandr Milshteyn**[5], **Dorothee Kern**[5], **Shmuel Muallem**[4], **Guo-li Ming**[1,2,3,^,#], and **Paul F. Worley**[3,#]

[1] Institute for Cell Engineering, Johns Hopkins University School of Medicine, 733 N. Broadway, Baltimore, MD 21205, USA

[2] Department of Neurology, Johns Hopkins University School of Medicine, 733 N. Broadway, Baltimore, MD 21205, USA

[3] The Solomon H. Snyder Department of Neuroscience, Johns Hopkins University School of Medicine, 725 N. Wolfe Street, Baltimore, MD 21205, USA

[4] Department of Physiology, University of Texas, Southwestern Medical Center, Dallas, TX 75390, USA

[5] Department of Biochemistry, Howard Hughes Medical Institute, Brandeis University, Waltham, MA 02452, USA

Summary

Immunophilins, including FK506-binding proteins (FKBPs), are protein chaperones with peptidyl-prolyl isomerase (PPIase) activity. Initially identified as pharmacological receptors for immunosuppressants to regulate immune responses via isomerase independent mechanisms, FKBPs are most highly expressed in the nervous system where their physiological function as isomerases remains unknown. We demonstrate that FKBP12 and FKBP52 catalyze *cis/trans* isomerization of regions of TRPC1 implicated in controlling channel opening. FKBP52 mediates stimulus-dependent TRPC1 gating through isomerization, which is required for chemotropic turning of neuronal growth cones to netrin-1 and myelin-associated glycoprotein and for netrin-1/DCC-dependent midline axon guidance of commissural interneurons in the developing spinal cord. By contrast, FKBP12 mediates spontaneous opening of TRPC1 through isomerization and is not required for growth cone responses to netrin-1. Our study demonstrates a novel physiological function of proline isomerases in chemotropic nerve guidance through TRPC1 gating and may have significant implication in clinical applications of immunophilin-related therapeutic drugs.

^Correspondence should be addressed to: Guo-li Ming, M.D. and Ph.D., Institute for Cell Engineering, Department of Neurology, Johns Hopkins University School of Medicine, 733 N. Broadway, BRB 729, Baltimore, MD 21205, USA, Tel: 443-287-7498; Fax: 410-614-9568, gming1@jhmi.edu.
*, #These authors contribute equally

Publisher's Disclaimer: This is a PDF file of an unedited manuscript that has been accepted for publication. As a service to our customers we are providing this early version of the manuscript. The manuscript will undergo copyediting, typesetting, and review of the resulting proof before it is published in its final citable form. Please note that during the production process errors may be discovered which could affect the content, and all legal disclaimers that apply to the journal pertain.

NIH-PA Author Manuscript
NIH-PA Author Manuscript
NIH-PA Author Manuscript

NIH-PA Author Manuscript

NIH-PA Author Manuscript

NIH-PA Author Manuscript

Introduction

FK506-binding proteins (FKBPs) and cyclosporine-binding cyclophilins are immunophilins with peptidyl-prolyl isomerase (PPIase) activity (Barik, 2006; Fischer et al., 1989; Gothel and Marahiel, 1999; Harding et al., 1989; Siekierka et al., 1989; Snyder et al., 1998; Takahashi et al., 1989). These isomerases catalyze the isomerization of prolyl-peptide bonds between *cis* and *trans* conformation, which can be a rate-limiting process that influences protein folding and function (Gothel and Marahiel, 1999). Immunophilins were originally discovered as biological receptors for commonly used immunosuppressant drugs FK506 (Harding et al., 1989; Siekierka et al., 1989) and cyclosporine A (Fischer et al., 1989; Takahashi et al., 1989), respectively. Though both cyclosporine A and FK506 inhibit the PPIase activity of immunophilins, their immunosuppressive function is isomerase activity-independent and instead results from inhibition of calcineurin by the cyclophilins-cyclosporine A or FKBP-FK506 complex (Liu et al., 1991). Interestingly, FKBPs are 10–50 times more enriched in the nervous system than in the immune system (Steiner et al., 1992). Previously, limited studies of FKBPs in the nervous system have been largely focused on their roles as calcineurin inhibitors in association with FK506 and as protein chaperones, functions that are independent of the isomerase activity (Barik, 2006; Snyder et al., 1998). While important in clinical applications, these drug-dependent gain-of-function properties of FKBPs are not indicative of the physiological relevance since mammalian cells do not naturally encounter immunosuppressant drugs. The endogenous cellular functions of PPIases and their substrates in the nervous system remain elusive.

Advances in the medicinal chemistry of FK506 have led to the discovery of agents that specifically inhibit the PPIase activity of FKBPs, but do not inhibit calcineurin. These compounds, such as GPI-1046, while not immunosuppressive, provide a tool to examine the physiological function of FKBPs as isomerases independent of calcineurin. GPI-1046 was reported to enhance neuronal outgrowth following injury (Burnett and Becker, 2004; Guo et al., 2001). Despite their initial promise, the utility of these compounds has been limited, in part because of the uncertainty of their molecular target and basis of action. Notably, there is a poor correlation between the efficacy of inhibiting the PPIase activity of FKBP12 and promotion of axonal outgrowth (Gold et al., 1999). Moreover, the efficacy of PPIase inhibitors is not diminished in neurons cultured from FKBP12 knockout mice (Guo et al., 2001), suggesting the existence of additional targets. GPI-1046 was also reported to protect neurons from lethal effects of HIV-1 proteins TAT and gp120 by reducing the Ca^{2+} load in endoplasmic reticulum, suggesting a link with Ca^{2+} signalling (Caporello et al., 2006).

The FKBP family member FKBP52 recently has been reported to bind TRPC1 cation channels (Sinkins et al., 2004). FKBP52 is similar to FKBP12 in that it contains an N-terminal PPIase domain that binds FK506 and GPI-1046, but also possesses a second PPIase-like domain that lacks catalytic activity, three tetratricopeptide repeat domains that mediate specific protein interactions, and a C-terminal calmodulin binding site (Davies and Sanchez, 2005). TRPCs are six membrane spanning cation channels that belong to the TRP superfamily of proteins, which mediate diverse cellular sensory responses (Clapham, 2003; Nilius et al., 2007; Venkatachalam and Montell, 2007). Notably, TRPC1 mediates Ca^{2+} influx and subsequent growth cone turning responses to netrin-1 in vitro (Shim et al., 2005; Wang and Poo, 2005) and is required for midline axon guidance of commissural interneurons in the developing spinal cord in vivo (Shim et al., 2005). TRPC1-dependent Ca^{2+} signaling has also been implicated in mediating neuronal responses to myelin and glia scar-associated inhibitors that prevent axonal regeneration in the adult central nervous system and is necessary for growth cone responses of *Xenopus* spinal neurons to myelin-associated glycoprotein (MAG)(Shim et al., 2005). In support of a role for FKBPs in TRPC channel opening, FK506 disrupts FKBP-TRPC binding and inhibits TRPC6 channel activity (Sinkins et al., 2004). Since FK506 disrupts both the

NIH-PA Author Manuscript

NIH-PA Author Manuscript

NIH-PA Author Manuscript

binding and PPIase activity, and also inhibits calcineurin, the mechanism by which FKBPs contribute to TRPC channel gating remains unknown. In *Drosophila*, a FKBP52 homolog associates with TRPL and inhibits Ca^{2+} influx (Goel et al., 2001). FKBP52 also inhibits TRPV5 activation and subsequent Ca^{2+} influx when co-expressed in HEK293 cells (Gkika et al., 2006). The role of FKBP isomerases in regulating TRP channels, in particular their PPIase function in vivo, remains to be determined.

In considering how FKBPs might impact the TRPC1 function, we noted that the C-terminal region of TRPC1 implicated in FKBP52 binding overlaps with the sites of physical interaction with Homer (Yuan et al., 2003) and STIM1 (Huang et al., 2006; Zeng et al., 2008), which regulate gating of TRPC1. Homer binding to TRP box 2 (Figure 1A) is essential for normal gating of TRPC1 and, in combination with its ability to self-associate and bind a second site in the N-terminus of TRPC1, Homer maintains the channel in a closed state that can be activated by G-protein receptors or depletion of intracellular Ca^{2+} stores (Yuan et al., 2003). Moreover, the two aspartate residues immediately N-terminal to TRP box 2 associate with the C-terminus of STIM1 to open the channel in response to depletion of intracellular Ca^{2+} stores (Zeng et al., 2008). The presence of the putative FKBP52 binding site in regions critical for TRPC1 gating suggested a possible role for FKBP52 in channel opening. Here, we report that FKBP52 regulates the agonist-dependent opening of TRPC1 channels whereas FKBP12 stimulates spontaneous opening, both in a PPIase-dependent fashion. Furthermore, FKBP52 PPIase activity is selectively required for normal growth cone responses to specific guidance cues both in vitro and in vivo. Our study demonstrates a novel function of PPIases in chemotropic nerve guidance through gating of TRPC1 channel activity.

Results

FKBP52 binds regions of TRPC1 that are important for channel gating

To explore the role of FKBPs in regulating TRPC1 channel function, we first examined binding between FKBPs and TRPC1. As reported previously (Sinkins et al., 2004), TRPC1-WT (wild-type) co-immunoprecipitated (co-IP) with native FKBP52 in HEK293 cells (Figure 1B). Point mutations of TRPC1 in the TRP box 2, including TRPC1-P645L, P646L and F648R, disrupted the co-IP of TRPC1 with FKBP52 (Figures 1A and 1B). The dependence of binding upon P645 is consistent with the consensus binding site for the FKBP family PPIases that typically includes a hydrophobic amino acid (L644) followed by a proline (Schiene-Fischer and Yu, 2001). TRPC1 mutations with defective FKBP52 binding also disrupted their binding to Homer 3 (H3; Figure 1B), suggesting that FKBP52 and Homer bind to the same region in TRPC1. We also identified point mutations of TRPC1 that bound FKBP52 but not Homer (including TRPC1-L644S, L644A and P645A; Figure 1B), suggesting that they have overlapping but distinct sites of interaction. In addition, the newly created 645A-646P in the TRPC1-P645A mutant might be able to substitute for the natural binding site for it's binding to FKBP52. We did not identify TRPC1 mutants that bound Homer but not FKBP52.

The N-terminal Homer binding site also includes a consensus sequence for FKBP interaction (Figure 1A). Point mutations in the N-terminus of the full-length TRPC1 that disrupt its co-IP with Homer (Yuan et al., 2003) did not alter TRPC1 co-IP with FKBP52 (Figure S1). Since FKBP52 binding to the C-terminus of TRPC1 could obscure effects of mutations in the N-terminus, we repeated binding studies using an N-terminal fragment of TRPC1 (TRPC1-NT). Pull down experiments showed that GST-FKBP52 bound WT-TRPC1-NT (Figure 1C). Analysis of mutations of TRPC1 revealed that TRPC1-NT-P23A bound GST-FKBP52, whereas TRPC1-NT-L19A and TRPC1-NT-P20A did not. These results indicate that, similar to the C-terminal region, FKBP52 and Homer bind overlapping but distinct sites in the N-terminal region of TRPC1. In contrast to FKBP52, we did not detect FKBP12 binding to TRPC1 using co-IP or GST pull-down assays (data not shown).

NIH-PA Author Manuscript

NIH-PA Author Manuscript

NIH-PA Author Manuscript

FKBP12 and FKBP52 catalyze cis/trans isomerization of L-P bonds in N- and C-terminal sequences of TRPC1

To directly examine whether FKBPs catalyze cis/trans isomerization of regions of TRPC1 that are implicated in channel opening, we used nuclear magnetic resonance (NMR) exchange spectroscopy to identify conformational exchange processes between states with different chemical shifts that occur in a 0.1 to 10s time regime (Macura et al., 1994; Perrin and Dwyer, 1990), including *cis*/*trans* isomerization (Bosco et al., 2002; Kern et al., 1993). We generated ^{15}N-labelled TRPC1(14–30) and TRPC1(635–656) peptides that include the FKBP52 binding sites from N- and C- termini of TRPC1, respectively. Due to the spectral overlap, TRPC1(14–30) had to be specifically ^{15}N-labelled at the single Leu residue only, while TRPC1(635–656) was uniformly ^{15}N-labelled.

Isomerization around L-P bonds corresponding to the L19-P20 and L644-P645 positions in the full length TRPC1 was slow on the NMR timescale ($< 0.1\ s^{-1}$), as shown by distinct amide resonance signals corresponding to *cis* and *trans* conformations in approximately 1:10 ratio consistent with thermodynamically expected distribution of the two conformers for an unstructured peptide (Reimer et al., 1997) (Figure 1D). To assess the effect of FKBPs on TRPC1, we performed 2-dimentional ^{1}H-^{15}N heteronuclear exchange experiments (Farrow et al., 1994) on ^{15}N-labelled TRPC1(14–30) and TRPC1(635–656) peptides in the presence of catalytic amounts of recombinant FKBP12 or FKBP52. Addition of FKBP12 or FKBP52 to either peptide resulted in the appearance of exchange peaks connecting L19 and L644 *cis* and *trans* auto peaks, and a corresponding reduction in the intensity of the auto peaks (Figure 1D). These results demonstrated that both FKBP12 and FKBP52 efficiently catalyze the *cis*/*trans* isomerization about L-P bonds in N- and C-terminal regions of TRPC, with the N-terminal site being catalyzed with > 4.5 fold efficiency relative to the C-terminal site. It is notable that FKBP12 was catalytically effective despite the absence of biochemically-defined binding in co-IP or GST-pull-down assays, which is consistent with the notion that catalysis does not require high-affinity binding.

We also used NMR to evaluate point mutants FKBP12-D37L and FKBP52-FD67DV for their ability to catalyze isomerization of TRPC1 peptides (Figure S2). Both mutants have been previously reported to possess reduced catalytic activity toward artificial substrates (Barent et al., 1998; Tradler et al., 1997). Addition of either of the FKBP mutants at molar ratios as high as 1:5 relative to the TRPC1 peptides, which was significantly higher than those used with WT FKBPs, failed to produce significant exchange, indicating at least an order of magnitude reduction in catalytic activity relative to WT FKBPs (Figure S2). In biochemical assays, FKBP52-FD67DV bound TRPC1 N- and C-terminal regions similarly to FKBP52-WT, and like FKBP12-WT, FKBP12-D37L did not bind TRPC1 (data not shown).

Taken together, these results identified TRPC1 as an endogenous PPIase substrate of FKBP52 and FKBP12.

FKBP52 and FKBP12 PPIase activity differentially regulate TRPC1 channel opening

We next examined the role of FKBPs on TRPC1 channel gating using electrophysiology. To distinguish between effects of binding versus PPIase activity, we included FKBP52-FD67DV and FKBP12-D37L in our assays. Initial analysis determined that WT and PPIase-inactive FKBPs did not substantially alter TRPC1 trafficking to the plasma membrane of HEK293 cells. Both WT and PPIase-inactive mutants of FKBPs increased surface TRPC1 by ~2 fold (Figure S3). FKBP transgene expression did not alter the physical association of TRPC1 with IP_3R (Figure S3), which has been implicated in channel opening (Kiselyov et al., 1999). Similarly, FKBPs did not alter the association of Homer and IP_3R (Figure S3), which may be important for internal Ca^{2+} release (Mikoshiba, 2007). Recordings of TRPC1 currents from the same

NIH-PA Author Manuscript

NIH-PA Author Manuscript

NIH-PA Author Manuscript

preparation, however, showed striking differences in the spontaneous and agonist-induced currents (Figure 2). In the absence of FKBP transgene, TRPC1 produced a small spontaneous current (with a nearly linear I/V) that increased ~ 4 folds upon stimulation of transfected M3 receptors with 100 μM carbachol (Figures 2A and 2D). Co-expression of FKBP12 resulted in ~ 2 folds increase in the total current, most of which was spontaneously active and was not further increased by stimulation with carbachol (Figures 2B and 2D). Co-expression of FKBP52 also resulted in ~ 2.5 folds increase of the total current (Figures 2C and 2D). In contrast to FKBP12, the major effect of FKBP52 was to increase the agonist-stimulated current with little effect on the spontaneous current (Figures 2C and 2D). Notably, effects of both FKBPs were dependent on their PPIase activity since FKBP12-D37L and FKBP52-FD67DV blocked both spontaneous and carbachol-induced currents (Figures 2B, 2C and 2D). These observations indicate that FKBP52 amplifies the receptor-regulated activity of TRPC1 channel in a PPIase activity-dependent fashion.

To gain further insight into the molecular mechanism of FKBP52 in TRPC1 channel opening, we monitored its action on a panel of TRPC1 mutants. TRPC1-P23A, which binds FKBP52 but not Homer (Figures 1C and S1), showed a large spontaneous current with little agonist-stimulated response (Figure 2E), consistent with a model in which Homer must bind to both the N- and C-terminal sequences to prevent spontaneous channel activity (Yuan et al., 2003). Over-expression of FKBP52 resulted in a reduction of spontaneous current and an increase of agonist-stimulated current. This result is consistent with the notion that FKBP52, like Homer, can prevent spontaneous channel activity by binding both N- and C-termini of TRPC1. Similarly, TRPC1-P645A, which binds FKBP52 but exhibits reduced binding to Homer (Figure 1B), showed large spontaneous and low agonist-stimulated current, and was restored to near WT function by over-expression of FKBP52 (Figure 2E). By contrast, TRPC1-F648R, which does not bind Homer or FKBP52, showed a large spontaneous current that was not altered upon over-expression of FKBP52 (Figure 2E). Like FKBP52, FKBP12 increased the total current of TRPC1-WT; however, FKBP12 did not reduce spontaneous current or restore agonist-stimulated channel properties to TRPC1-P23A or TRPC1-P645A (data not shown). Since FKBP12 does not bind TRPC1 in biochemical assays, the differential effects of FKBP52 and FKBP12 are consistent with a model that FKBP52 binding to both N- and C-termini of TRPC1 is required to prevent spontaneous channel activity. Importantly, restoration of the mutant channel activity by FKBP52-WT, but not FKBP52-FD67DV, further suggests an essential role for PPIase activity for TRPC1 channel opening.

Netrin-1-induced Ca^{2+} rise in neuronal growth cones requires PPIase activity of FKBP52

FKBP52 is highly expressed in the developing nervous system of *Xenopus* embryos (Figure S4A) and is conserved across vertebrate species (Figure S4B). *Xenopus* TRPC1 (XTRPC1) is a critical mediator of netrin-1-induced Ca^{2+} influx and attractive growth cone guidance (Shim et al., 2005; Wang and Poo, 2005). As reported previously (Ming et al., 2002; Wang and Poo, 2005), netrin-1 induced significant rise of intracellular Ca^{2+} ($[Ca^{2+}]_i$) within growth cones of cultured *Xenopus* spinal neurons (Figures 3A, 3D and 3E). This $[Ca^{2+}]_i$ rise requires netrin-1 receptor DCC, since a specific morpholino against *Xenopus* DCC (XDCC-MO) abolished the netrin-1-induced $[Ca^{2+}]_i$ rise (Figures 3D and 3E). Inhibition of PPIase activity by GPI-1046 (Figure 3B) or expression of FKBP52-FD67DV (Figure 3C) also abolished netrin-1-induced $[Ca^{2+}]_i$ rise in growth cones (Figures 3D and 3E). Furthermore, over-expression of TRPC1-P645L, which is constitutively active (Yuan et al., 2003), prevented the ability of netrin-1 to evoke an increase of $[Ca^{2+}]_i$ (Figure 3E), consistent with the electrophysiology result that the constitutive activity of TRPC1-P645L cannot be increased by agonist stimulation (Yuan et al., 2003).

NIH-PA Author Manuscript

NIH-PA Author Manuscript

NIH-PA Author Manuscript

Netrin-1-induced attractive growth cone turning requires PPIase activity of FKBP52

Ligand-induced Ca^{2+} influx in the growth cone is essential for guidance responses to a group of guidance cues (Hong et al., 2000; Zheng, 2000). We assessed the functional role of FKBP52 in axon guidance using a well-established in vitro growth cone turning assay (Lohof et al., 1992; Ming et al., 1997; Ming et al., 2002; Song et al., 1998; Zheng et al., 1994). In a microscopic gradient of netrin-1, *Xenopus* spinal neurons exhibited chemoattractive growth cone turning responses (Figure 4A). When these growth cones were exposed to a netrin-1 gradient in the presence of FK506 or GPI-1046, attractive growth cone turning responses were completely abolished (Figures 4B, 4C and 4E), consistent with their inhibition of netrin-1-induced $[Ca^{2+}]_i$ rise (Figure 3). Similarly, expression of FKBP52-FD67DV, but not FKBP52-WT, blocked netrin-1-induced attraction (Figures 4D and 4E). Furthermore, specific morpholinos against *Xenopus* FKBP-52 (XFKBP52-MO), but not a control morpholino, blocked attractive growth cone turning responses to netrin-1 (Figure S5). Thus, FKBP52 PPIase activity is required for netrin-1-induced attraction.

We sought to determine whether the action of FKBP52 on TRPC1 is required for mediating netrin-1-induced attraction or whether they only create a permissive condition for a different signal to induce turning. We noted that axons continued to grow in the presence of FKBP inhibitors or expression of FKBP and TRPC mutants that blocked attractive responses to netrin-1, indicating that general axonal growth was not impaired. Next, we examined effects of expression of TRPC1-P645L and TRPC1-P645A. Since both of these channels are constitutively open, if the action of FKBP52 on the opening of TRPC1 provides a permissive condition, both channels would be expected to support attractive responses. However, expression of either TRPC1-P645L or TRPC1-P645A abolished netrin-1-induced attraction (Figure 4F). Moreover, over-expression of FKBP52-WT with TRPC1-P645A rescued netrin-1-induced attraction (Figure 4F), in a manner that parallels FKBP52-dependent conversion of TRPC1-P645A constitutive activity to induced activity in HEK293 cells (Figure 2E). These data support a model in which FKBP52 action on TRPC1 is required for netrin-1-induced attraction, instead of a permissive role. Interestingly, expression of FKBP12-WT or FKBP12-D37L did not affect attractive turning responses to a netrin-1 gradient (Figure S6), which reinforces the specific role of FKBP52 and TRPC1 activity in netrin-1 signalling.

Growth cone chemoattraction requires a local gradient of a ligand that is thought to differentially activate receptors and downstream signal cascades for the biased growth toward higher concentration gradient (Figure 4G) (Ming, 2006). If the PPIase activity of FKBP52 is sufficient for the signalling output of netrin-1, then our model predicts that a local gradient of PPIase activator should be able to induce attractive turning responses even in the absence of a netrin-1 gradient. The model further predicts that growth cones should turn away from a local PPIase inhibitor gradient in the presence of uniform activation of PPIase activity by bath application of netirn-1, given netrin receptor-dependent PPIase signalling should be reduced on the side facing higher concentration of inhibitors (Figure 4G). Because of a lack of specific PPIase activators, we tested our model using PPIase inhibitor GPI-1046. We subjected growth cones to a gradient of GPI-1046 (100 μM in the pipette) with concurrent, uniform netrin-1 activation (10 ng/ml in the bath). Consistent with the model, neuronal growth cones exhibited significant turning responses away from the PPIase inhibitor (Figure 4H). This effect was not due to the general inhibition of axonal outgrowth by GPI-1046, since neurons in the same GPI-1046 gradient without uniform netrin-1 stimulation exhibited no change in the growth rate and importantly, no bias in the direction of growth cone extension (Figure 4H). Taken together, these results support the model that FKBP52 and TRPC1 signalling is both necessary and sufficient for netrin-1-induced growth cone steering in vitro.

NIH-PA Author Manuscript

NIH-PA Author Manuscript

NIH-PA Author Manuscript

FKBP52 and its regulation of TRPC1 are essential for commissural axon guidance in vivo

We next examined whether PPIase activity of FKBP52 is required for axon guidance in vivo. Netrin-1/DCC signalling is known to guide commissural axons to the CNS midline in the developing spinal cord of mouse (Figure 5A) (Serafini et al., 1996). To confirm a role for netrin-1/DCC signalling in development *Xenopus* spinal cord, we injected a specific morpholino against XDCC into *Xenopus* embryos at the one-cell stage and examined stage 25 embryos, a time when commissural interneuron axons have already reached the CNS midline (Shim et al., 2005). Commissural interneuron axons in developing *Xenopus* embryos were specifically identified with the 3A10 monoclonal antibody (Moon and Gomez, 2005; Phelps et al., 1999; Serafini et al., 1996; Shim et al., 2005) (Figure 5B; See Supplementary Movie 1). Many of the $3A10^{+}$ axons in embryos with XDCC-MO failed to reach the midline; instead, they joined ipsilateral tracts or turned longitudinally between the ipsilateral tract and the midline (Figure 5C; Supplementary Movie 2). Interestingly, some of commissural axons also lost contact avoidance and exhibited fasciculation prematurely before crossing the midline (Figure 5C) (Moon and Gomez, 2005). Thus, netrin-1/DCC-dependent midline guidance is functionally conserved in the developing *Xenopus* embryonic spinal cord.

Next, we applied GPI-1046 or FK506 to developing *Xenopus* embryos between stage 22–25, a time window when commissural interneuron axons are attracted to the midline (Shim et al., 2005). Such treatments led to significant guidance defects similar as those with XDCC-MO (Figures 5D, 5E and 5H). Over-expression of FKBP52-FD67DV, but not FKBP52-WT, led to similar midline targeting errors and premature fasciculation (Figures 5F, 5G and 5H; Supplementary Movie 3). Strikingly, some of the commissural neurons expressing FKBP52-FD67DV appeared to completely ignore guidance cues and send long projections outside of the spinal cord (Supplementary Movie 3).

To examine whether the interaction of TRPC1 and FKBP52 is essential for axon guidance in vivo, we manipulated the expression of TRPC1 and FKBPs. Consistent with our in vitro findings from the growth cone turning assay, expression of TRPC1-P645L or TRPC1-P645A led to significant midline guidance defects (Figures 6B, 6C and 6G; Supplementary Movie 4 and 5), very similar to those resulting from XDCC knockdown and inhibition of FKBP52 PPIase activity (Figure 5). Over-expression of FKBP52-WT, but not FKBP12-WT, largely rescued the guidance defect by TRPC1-P645A mutation (Figures 6D, 6E and 6G; Supplementary Movie 6 and 7). Also consistent with in vitro results, over-expression of FKBP12-WT or FKBP12-D37L alone did not result in altered guidance phenotypes (Figures 6F and 6G), again indicating the specific role of FKBP52. Taken together, these results demonstrate that PPIase-dependent regulation of TRPC1 channel activity specifically by FKBP52 is required for commissural interneuron axon guidance in the developing *Xenopus* spinal cord in vivo.

Repulsive growth cone responses to MAG, but not Sema3A, requires PPIase activity of FKBP52

MAG is a major component of myelin (McKerracher et al., 1994; Mukhopadhyay et al., 1994), and we previously showed that MAG-induced repulsion of growth cones of *Xenopus* spinal neurons requires the function of XTRPC1 (Shim et al., 2005). Similar to *Xenopus* spinal neurons, axonal growth cones of rat hippocampal neurons exhibited significant repulsive turning responses to a MAG gradient (Figure 7A) (Goh et al., 2008). Interestingly, application of GPI-1046 or over-expression of FKBP52-FD67DV abolished MAG-induced repulsion in these mammalian neurons (Figures 7A and 7B). Furthermore, over-expression of TRPC1-P645A, which shows constitutive channel activity (Figure 2E), blocked MAG-induced growth cone repulsion (Figures 7A and 7B). Importantly, co-expression of FKBP52-WT and TRPC1-P645A rescued MAG-induced repulsion in these neurons (Figure 7B). Thus, proline

NIH-PA Author Manuscript

NIH-PA Author Manuscript

NIH-PA Author Manuscript

isomerization of TRPC1 by FKBP52 is essential for transducing MAG signalling in mammalian neurons.

To further examine the specificity of PPIase in growth cone guidance, we examined repulsive turning responses of *Xenopus* spinal neurons to a Sema3A gradient, which were known to be independent Ca^{2+} and TRPC1 (Shim et al., 2005). Interestingly, bath application of either FK506 or GPI-1046 exhibited no significant effects on Sema3A-induced repulsive growth cone turning responses (Figure 7C). Taken together, these results indicate that PPIase activity of FKBP52 is selectively required for growth cone response to guidance cues involving Ca^{2+} and TRPC1 signalling.

Discussion

Using biochemistry, NMR, electrophysiology, Ca^{2+} imaging and functional axon guidance assay, we demonstrated that the isomerase activity of FKBP52 regulates neuronal growth cone responses to netrin-1 both in vitro and in vivo through regulation of TRPC1 channel opening. The present finding identifies an isomerase-dependent physiological and endogenous function of immunophilins in the biological system in vivo. The PPIase-dependent molecular mechanism is likely to be broadly relevant to TRPC channel gating, and we demonstrate that it underlies attractive neuronal growth cone responses to netrin-1 in *Xenopus* neurons and repulsive responses to MAG in mammalian neurons. Both of these responses have been previously characterized to be dependent on $[Ca^{2+}]_i$ and TRPC1 (Shim et al., 2005). In contrast, repulsive growth cone responses to Sema3A, which were known to be independent Ca^{2+} and TRPC1 (Shim et al., 2005), is not regulated by the PPIase activity. Previous studies have established that netrin-1 induces an attractive response upon its binding to DCC, which signals in a manner that is dependent on increased $[Ca^{2+}]_i$, cAMP, activation of phospolipase C-γ (PLC-γ), PI3K, MAPK and Rho GTPases (Song and Poo, 1999). While the mechanism of coupling between DCC and TRPC1 is not known, PLC-γ is implicated in TRPC3 activation in neuronal growth cone responses to BDNF (Li et al., 2005). The present study indicates that for its normal function, TRPC1 activation is coupled to netrin-1/DCC signalling via isomerization by FKBP52, since expression of constitutively active TRPC1 mutants blocked both the netrin-1-induced increase of $[Ca^{2+}]_i$ and growth cone attraction, and these responses were rescued by co-expression of FKBP52 that restores agonist-dependent TRPC1 channel activity. Failure of FKBP12 and FKBP12-D37L to alter netrin-1-dependent responses in neurons contrasts with experiments in HEK293 cells expressing transgene M3 receptor and TRPC1, and suggests that the native netrin-1/DCC signaling complex is selective for FKBP52.

Our studies provide novel molecular insight into how FKBP52 might confer agonist-dependent opening of TRPC1. Previous studies on the regulation of TRPC1 by Homer suggests that physical interactions linking discrete regions in the N- and C-terminus of TRPC1 prevent spontaneous channel activity (Yuan et al., 2003). Disruption of Homer binding, or of Homer's ability to self-associate, results in spontaneous TRPC1 channel activity. FKBP52 binds N- and C-terminal regions of TRPC1 that overlap with the binding sites for Homer. Like Homer, FKBP52 can dimerize, an activity that is dependent on the N-terminal PPIase domain (Davies and Sanchez, 2005), and FKBP52 can restore agonist-dependent channel opening of TRPC1 mutants that fail to bind Homer. FKBP52 is distinct from Homer in that it possesses the PPIase activity essential for channel opening. FKBP52 accelerates isomerization of L-P bonds in both the N- and C-terminal sequences; however, the relationship between isomerization of these specific bonds and channel opening remains to be determined. The observation that FKBP12 also accelerates isomerization and increases channel activity, but does not tightly bind or confer agonist-dependent channel opening, supports the notion that the ability of FKBP52 to tightly bind TRPC1 is important for stimulus-dependent regulation. Importantly, the physiological action of FKBP52 is fundamentally different from the action of FKBP12, which increases the

NIH-PA Author Manuscript

NIH-PA Author Manuscript

NIH-PA Author Manuscript

spontaneous channel opening of TRPC1. Additional studies are required to fully understand the individual and cooperative actions of FKBPs, Homer and STIM1 in TRPC1 channel gating.

Immunosuppressant drugs, such as FK506, are widely used to treat patients with autoimmune disorders and to prevent rejection of organ transplants. We have identified TRPC1 as an endogenous substrate of PPIase activity of FKBPs. Our study raises a potential concern that immunosuppressant drugs might affect fetal nervous system development. Indeed, increased abortion rate and pre-term delivery has been noted for patients using immunosuppressant drugs during pregnancy (Miniero et al., 2002). On the other hand, given the observed dependence of MAG signalling on the PPIase activity of FKBP52, the differential physiological function of FKBP12 versus FKBP52 identified in our study may be therapeutically relevant. Accordingly, FKBP52 may provide a rational target for new medicinal chemistry directed toward promotion of axonal regeneration and neural protection in the adult central nervous system.

Experimental Procedures

Reagents and transfection

TRPC1 and Homer3 constructs were described previously (Xiao et al., 1998; Yuan et al., 2003). FKBP12 and FKBP52 constructs were generously provided by A. Srivastava (University of Florida). Point mutations were generated by site-directed mutagenesis (Stratagene). The antibodies used were monoclonal anti-myc and HRP-conjugated anti-myc and anti-HA (all from Santa Cruz Biotech), rabbit polyclonal anti-Homer 3 (Xiao et al., 1998), monoclonal anti-IP_3 receptor type 3 (for co-IP; BD Biosciences), goat polyclonal anti-pan-IP_3 receptor (for Western blot; gift from A. Sharp), and rabbit polyclonal anti-FKBP59/FKBP52 (Affinity BioReagents). Plasmid transfection was done using calcium phosphate for 6 hrs, washed once with 1X PBS, and replaced with regular HEK293 media. Cells were incubated at 37°C for 36–48 hrs. The amount of cDNA transfected in a 100-mm dish was 10 μg or less. These cells were used for electrophysiology and co-IP analysis the following day.

Biochemistry

Protein binding assays were done as previously described (Yuan et al., 2003). Transfected cells were harvested and lysed using 500 μl of binding buffer: 1X PBS buffer containing 1 mM $NaVO_3$, 10 mM NaPyrophosphate, 50 mM NaF [pH 7.4], and 1% Triton X-100. The cell extracts were sonicated, and insoluble material was spun down at 30,000g for 20 min. For GST pull-down, GST-FKBP52 was expressed in BL21 bacterial cells by growing a 400 ml culture at 37°C until A595 was 0.4–0.6. Cells were induced with 125 mM IPTG for an additional hour, harvested, lysed in 10 μl of 1% Triton X-100 in 1X PBS with 200 mg/ml PMSF, sonicated 3 × 10 strokes, and spun down at 12,000g for 5 min. The supernatant was mixed 1:1 with slurry of GST-agarose beads (Sigma) for 30 min at 4°C. Beads were washed 2 times with 1% Triton X-100 in 1X PBS and 2 times with 1X PBS. 50 μl of 1:1 slurry of GST-FKBP52 beads were used per 100 μl cell extract and rocked for 2 hrs at 4°C. For co-IP experiments, 1 μg of purified antibody or 2 μl of crude antiserum was added to 100 μl of cell extract and incubated for 1 hr at 4°C. Then, 1:1 slurry of protein A or G sepharose 4B beads were added to the antibody-extract mix and incubated for an additional hour at 4°C. Beads were washed 3 × 10 min with binding buffer, and proteins were released from the beads with SDS-loading buffer and subjected to Western blot analysis.

For biotinylation assay, transfected cells were washed once with 1X PBS on ice. EZ-Link Sulfo-NHS-SS-Biotin (0.5 mg/ml; Pierce) was added to the cells for 30 mins on ice. Afterwards, the biotin was quenched with 50 mM glycine on ice for 10–15 min. The cells were then processed as described above to make cell extract. 50 μl of 1:1 slurry of immobilized avidin beads (Pierce) were added to 100 μl of cell extract and incubated for 2 hrs at 4°C. Beads

NIH-PA Author Manuscript

NIH-PA Author Manuscript

NIH-PA Author Manuscript

were washed 3 × 10 mins with binding buffer and proteins were released from the beads with SDS-loading buffer and subjected to Western blot analysis.

NMR Sample Preparation and Data Collection

Vectors for expression of TRPC1(14–30) and TRPC1(635–656) peptides were constructed as GB1 fusion proteins using a modified QuikChange protocol (Stratagene) to insert peptide sequences into pET30a vector containing GB1 with C-terminal 6xHis-tag cleavable with TEV protease (original vector containing GB1 expression construct was a generous gift of G. Wagner, Harvard Medical School). Following proteolytic cleavage the peptides were comprised of the sequences corresponding to TRPC1(14–30) [GSHHHHHHGASSS**LP**SSPSSSSSPN] and to TRPC1(635–656) [GSHHHHHHLSYFDDKCT**LP**PPFNIIPSPKT]. Specifically, ^{15}N-Leu-labeled TRPC1(14–30) was prepared as previously described (Muchmore et al., 1989). Uniformly ^{15}N-labeled TRPC1(635–656) was expressed in minimal M9 media supplemented with $^{15}NH_4Cl$. GB1 fusion proteins were purified using Ni-Sepharose column (GE LifeSciences) equilibrated with 500 mM NaCl, 50 mM Tris (pH 8.0), 1μL/mL βME and eluted using 20–300 mM Imidazole gradient in the same buffer. Following purification, TRPC1 peptides were cleaved with AcTEV protease (Invitrogen) in 50 mM Tris, 0.5 mM EDTA, 2 mM DTT and purified over ACE 5 C18–300 reverse phase HPLC column (ACT) using 15–35% acetonitrile gradient in H_2O/0.1% trifluoroacetic acid. TRPC1 peptides were desolvated using CentriVap concentrator (Labconco) and reconstituted in H_2O.

All FKBP proteins were expressed in BL21(DE3) *E.coli* cells, induced with 1 mM isopropyl-β-D-thiogalactoside, and harvested after 3–4hrs. FKBP12 was purified using GSTrap column equilibrated with PBS buffer (pH 7.4) supplemented with 1μL/mL βME. GST-tag was cleaved with restriction grade Thrombin (Novagen) in 150 mM NaCl, 20 mM Tris (pH 8.4), 2.5 mM $CaCl_2$, 2 mM DTT and removed using GSTrap column followed by Benzamidine Sepharose column equilibrated with PBS buffer (pH 7.4) to remove Thrombin. FKBP52 was purified using Ni-Sepharose column equilibrated with 500 mM NaCl, 50 mM Tris (pH 8.0), 1μL/mL βME and eluted using 20–300 mM Imidazole gradient in the same buffer (all columns were purchased from GE LifeSciences). Finally, FKBP proteins were buffer exchanged into 40 mM HEPES buffer (pH 7.4), 5 mM TCEP.

NMR samples were prepared at ^{15}N TRPC1 peptide/FKBP molar ratios indicated. Final sample buffer contained 40mM HEPES (pH 6.8–7.1), 4 mM DTT, 5 mM TCEP, 10% D_2O. Two-dimensional (2D) ^{1}H-^{15}N heteronuclear exchange experiments (Farrow et al., 1994) were collected on Bruker Avance 800 MHz spectrometer at 25°C with mixing times varying from 0 ms to 600 ms. All NMR spectra were processed with NMRPipe (Delaglio et al., 1995) and visualized using NMRViewJ software (Johnson and Blevins, 1994).

Electrophysiology

TRPC1 current in HEK293 cells was measured with/without over-expression of WT or mutant FKBP12/FKBP52 in whole-cell current recording configuration, as described previously (Huang et al., 2006; Yuan et al., 2007). Briefly, the pipette solution contained (in mM) 140 CsCl, 2 $MgCl_2$, 1 ATP, 5 EGTA, 1.5 $CaCl_2$ (free Ca^{2+} at 70 nM) and 10 HEPES at pH 7.2 with CsOH, to eliminate K^+ current and prevent inhibition of the channels by high cytoplasmic Ca^{2+}. The bath solution contained (in mM) 140 NaCl or 140 NMDG-Cl, 5 KCl, 0.5 EGTA and 10 HEPES at pH 7.4 with NaOH or NMDG-OH. The current was measured by ramp from −100 mV to +100 mV for 400 ms every 4s at holding potential 0 mV. The current recorded at −100 mV was used to calculate current density as pA/pF. Multiple independent experiments were used to obtain the mean ± SEM. Statistical significance was assessed using Student's t-test.

NIH-PA Author Manuscript

NIH-PA Author Manuscript

NIH-PA Author Manuscript

Xenopus embryo injection and spinal neuron culture

Blastomere injections of morpholino oligos or mRNAs encoding TRPC1, FKBP52, FKBP12, or their mutant forms into early stages of *Xenopus* embryos and culturing of spinal neurons from these injected embryos were performed as previously described (Shim et al., 2005). Specifically, fertilized embryos were injected at one- or two-cell stage, with a mixture of the morpholino (10 ng/embryo) or mRNA (2–3 ng/embryo), and a lineage tracer. The following DNA constructs were subcloned into the pCS2 vector (gif of D. Turner, University of Michigan) and used for in vitro transcription with the mMESSAGE mMACHINE SP6 kit (Ambion): Myc-FKBP52-WT, Myc-FKBP52-FD67DV, Myc-FKBP12-WT, Myc-FKBP12-D37L, HA-TRPC1-WT, HA-TRPC1-P645L, HA-TRPC1-P645A, GFP-XTRPC1. A morpholino oligo directed against *Xenopus* DCC (XDCC-MO) was designed with the following sequence: 5′-CCAAGACAATTCTCCATATTTCAGC-3′. Because of the presence of two FKBP52 homologues in the *Xenopus*, two morpholino oligos directed against *Xenopus* FKBP52 (XFKBP52A, B-MO) were designed with the following sequences: (XFKBP52A) 5′-CGGTCTTCATCTCCTCGGCAGTCAT -3′; (XFKBP52B) 5′-CAGGCTTCATCTCGTCAGCAGTCAT -3′. Injected embryos at stage 22 were used for cultures of spinal neurons as previous described (Shim et al., 2005).

Whole-mount in situ hybridisation, immunostaining and confocal imaging

Full-length open reading frame region of XFKBP12 (accession no. AB006678) and the C-terminal open reading frame region of XFKBP52 (BamHI-stop codon fragment; accession number: NM_001091447) were used to generate each specific digoxigenin-UTP-labelled anti-sense and sense RNA probes. For whole-mount in situ hybridization, the labelled probes were detected with alkaline phosphatase-conjugated anti- digoxigenin antibody (Fab fragments) and visualized with the BM purple AP substrate (Roche Applied Science). For fluorescent in situ hybridization (FISH), cultures of spinal neurons from stage 22 embryos were fixed in 4% PFA, 4% sucrose in PBS for 30 minutes at RT and hybridization and subsequent immunofluorescent detection was performed as described previously (Leung et al., 2006) except that anti-digoxigenin antibody and Alexa Fluor 568 secondary antibody (Jackson ImmunoResearch, West Grove, PA) were used.

Embryos at stage 23–28 were fixed and processed for immunocytochemistry as previously described (Shim et al., 2005). Monoclonal antibody 3A10, specific for commissural interneurons (Phelps et al., 1999; Serafini et al., 1996), was obtained from the Developmental Studies Hybridoma Bank at the University of Iowa and used at a dilution of 1:100. Secondary antibodies were used at a dilution of 1:250. Confocal images of sagittal views of embryos were taken with a Zeiss LSM 510 META system and Z-series reconstructions were processed with the Zeiss LSM image acquisition program. A minimal of 10 embryos was examined for each condition. Statistical significance was assessed using the Bootstrap test.

Ca^{2+} imaging of cultured *Xenopus* spinal neurons

Ca^{2+} imaging of growth cones of *Xenopus* spinal neurons was carried out as previously described (Ming et al., 1997; Ming et al., 2002). Specifically, isolated *Xenopus* spinal neurons were loaded with Fluo-4 AM (2 μM, Molecular Probes) in the culture media without serum for 30 mins at the room temperature, and rinsed with the media for growth cone turning assay. Ca^{2+} imaging was performed using a Zeiss 510 META system equipped with a 20X objective (NA 0.8). Excitation was at 488 nm by argon laser and the emitted fluorescence was collected at 500–560 nm. Fluorescence and bright-field images were simultaneously acquired at every 30 seconds with a frame scan. The fluorescence intensity of each time point was measured over a fixed rectangular region of interest that covers the entire growth cone and normalized to the average fluorescence intensity that was measured during a 5 mins baseline period (prior to netrin-1 application).

NIH-PA Author Manuscript

NIH-PA Author Manuscript

NIH-PA Author Manuscript

Primary hippocampal neuronal cultures and transfection

Hippocampal neurons were isolated from postnatal rats (P3-P5) and were cultured on poly-L-lysine coated coverslips as previously described (Goh et al., 2008; Song et al., 2002). These neurons were transfected with the Amaxa transfection system following protocols from the manufacturer. Briefly, hippocampal neurons were isolated and 100 μl of nucleofector solution was added to resuspend the cell pellet. Different expression constructs (1–5 μg) for GFP, FKBP52-FD67DV, TRPC1-P645A or a combination of TRPC1-P645A and FKBP52-WT, were added to the cell suspension and then transferred to cuvettes for electroporation. The cells were cultured in DMEM with 10% fetal bovine serum for 24 hrs before changing to serum-free neurobasal medium (Goh et al., 2008).

Growth cone turning assay

Microscopic gradients of netrin-1 (10 μg/ml in the pipette), MAG (150 μg/ml in the pipette), Sema3A (50 μg/ml in the pipette) and GPI-1046 (100 μM in the pipette) were produced as previously described (Lohof et al., 1992; Ming et al., 1997; Ming et al., 2002; Zheng et al., 1994). Previous characterization showed that at 100 μm away from the pipette tip the concentration of factors is about 1000 fold lower than that in the pipette and there is a 5–10% concentration gradient across the width of the growth cone (Lohof et al., 1992; Zheng et al., 1994). *Xenopus* spinal neurons were used at 14 to 20 hrs after plating and neurons with the lineage-tracer were identified under fluorescent microscope and used for turning assay at the room temperature as previously described (Shim et al., 2005). GFP^+ hippocampal neurons were used at 48–72 hrs after plating and individual axon was identified as the longest neurite for turning assay at the room temperature as previously described (Goh et al., 2008). The turning angle was defined by the angle between the original direction of neurite extension and a straight line connecting the positions of the center of the growth cone at the onset and the end of the 30 min period. The rates of neurite extension were calculated based on the net neurite extension during the turning assay. Only those growth cones of isolated neurons with a net neurite extension > 5 μm over the 30-min period were included for analysis. Statistical significance was assessed using the Bootstrap test.

Supplementary Material

Refer to Web version on PubMed Central for supplementary material.

Acknowledgments

We would like to thank H. Song, A. Kolodkin, T. Dawson, and Ming laboratory members for comments and suggestions, N. Marsh-Armstrong for providing the frog facility, S. Andrabi for help with Ca^{2+} imaging. This work was supported by NIH (NIDA10309) to P.W., NIH (DE12309 and DK38938) and the Ruth S. Harrell Professorship in Medical Research to S.M., Howard Hughes Medical Institute and by NIH to D.K., and by NIH (NS0488271), March of Dimes, Alfred P. Sloan Foundation, Adelson Medical Research Foundation and Brain Science Institute at Johns Hopkins to G.L.M. J.Y.L. was partially supported by a postdoctoral fellowship from MSCRF.

References

Barik S. Immunophilins: for the love of proteins. Cell Mol Life Sci 2006;63:2889–2900. [PubMed: 17075696]

Bosco DA, Eisenmesser EZ, Pochapsky S, Sundquist WI, Kern D. Catalysis of cis/trans isomerization in native HIV-1 capsid by human cyclophilin A. Proc Natl Acad Sci U S A 2002;99:5247–5252. [PubMed: 11929983]

Clapham DE. TRP channels as cellular sensors. Nature 2003;426:517–524. [PubMed: 14654832]

Davies TH, Sanchez ER. Fkbp52. Int J Biochem Cell Biol 2005;37:42–47. [PubMed: 15381148]

NIH-PA Author Manuscript

NIH-PA Author Manuscript

NIH-PA Author Manuscript

Delaglio F, Grzesiek S, Vuister GW, Zhu G, Pfeifer J, Bax A. NMRPipe: a multidimensional spectral processing system based on UNIX pipes. J Biomol NMR 1995;6:277–293. [PubMed: 8520220]

Farrow NA, Zhang O, Forman-Kay JD, Kay LE. A heteronuclear correlation experiment for simultaneous determination of 15N longitudinal decay and chemical exchange rates of systems in slow equilibrium. Journal of biomolecular NMR 1994;4:727–734. [PubMed: 7919956]

Fischer G, Wittmann-Liebold B, Lang K, Kiefhaber T, Schmid FX. Cyclophilin and peptidyl-prolyl cis-trans isomerase are probably identical proteins. Nature 1989;337:476–478. [PubMed: 2492638]

Gkika D, Topala CN, Hoenderop JG, Bindels RJ. The immunophilin FKBP52 inhibits the activity of the epithelial Ca2+ channel TRPV5. Am J Physiol Renal Physiol 2006;290:F1253–1259. [PubMed: 16352746]

Goel M, Garcia R, Estacion M, Schilling WP. Regulation of Drosophila TRPL channels by immunophilin FKBP59. J Biol Chem 2001;276:38762–38773. [PubMed: 11514552]

Goh EL, Young JK, Kuwako K, Tessier-Lavigne M, He Z, Griffin JW, Ming GL. beta1-integrin mediates myelin-associated glycoprotein signaling in neuronal growth cones. Mol Brain 2008;1:10. [PubMed: 18922173]

Gold BG, Densmore V, Shou W, Matzuk MM, Gordon HS. Immunophilin FK506-binding protein 52 (not FK506-binding protein 12) mediates the neurotrophic action of FK506. J Pharmacol Exp Ther 1999;289:1202–1210. [PubMed: 10336507]

Gothel SF, Marahiel MA. Peptidyl-prolyl cis-trans isomerases, a superfamily of ubiquitous folding catalysts. Cell Mol Life Sci 1999;55:423–436. [PubMed: 10228556]

Harding MW, Galat A, Uehling DE, Schreiber SL. A receptor for the immunosuppressant FK506 is a cis-trans peptidyl-prolyl isomerase. Nature 1989;341:758–760. [PubMed: 2477715]

Hong K, Nishiyama M, Henley J, Tessier-Lavigne M, Poo M. Calcium signalling in the guidance of nerve growth by netrin-1. Nature 2000;403:93–98. [PubMed: 10638760]

Huang GN, Zeng W, Kim JY, Yuan JP, Han L, Muallem S, Worley PF. STIM1 carboxyl-terminus activates native SOC, I(crac) and TRPC1 channels. Nat Cell Biol 2006;8:1003–1010. [PubMed: 16906149]

Johnson BA, Blevins RA. NMR View: A computer program for the visualization and analysis of NMR data. Journal of biomolecular NMR 1994;4:603–614.

Kern D, Drakenberg T, Wikstrom M, Forsen S, Bang H, Fischer G. The cis/trans interconversion of the calcium regulating hormone calcitonin is catalyzed by cyclophilin. FEBS Lett 1993;323:198–202. [PubMed: 8500610]

Kiselyov K, Mignery GA, Zhu MX, Muallem S. The N-terminal domain of the IP3 receptor gates store-operated hTrp3 channels. Mol Cell 1999;4:423–429. [PubMed: 10518223]

Leung KM, van Horck FP, Lin AC, Allison R, Standart N, Holt CE. Asymmetrical beta-actin mRNA translation in growth cones mediates attractive turning to netrin-1. Nat Neurosci 2006;9:1247–1256. [PubMed: 16980963]

Li Y, Jia YC, Cui K, Li N, Zheng ZY, Wang YZ, Yuan XB. Essential role of TRPC channels in the guidance of nerve growth cones by brain-derived neurotrophic factor. Nature 2005;434:894–898. [PubMed: 15758952]

Liu J, Farmer JD Jr, Lane WS, Friedman J, Weissman I, Schreiber SL. Calcineurin is a common target of cyclophilin-cyclosporin A and FKBP-FK506 complexes. Cell 1991;66:807–815. [PubMed: 1715244]

Lohof AM, Quillan M, Dan Y, Poo MM. Asymmetric modulation of cytosolic cAMP activity induces growth cone turning. J Neurosci 1992;12:1253–1261. [PubMed: 1372932]

Macura, S.; Westler, WM.; Markley, JL.; Thomas, LJ.; Norman, JO. Methods in Enzymology. Academic Press; 1994. Two-dimensional exchange spectroscopy of proteins; p. 106-144.

McKerracher L, David S, Jackson DL, Kottis V, Dunn RJ, Braun PE. Identification of myelin-associated glycoprotein as a major myelin-derived inhibitor of neurite growth. Neuron 1994;13:805–811. [PubMed: 7524558]

Mikoshiba K. IP3 receptor/Ca2+ channel: from discovery to new signaling concepts. J Neurochem 2007;102:1426–1446. [PubMed: 17697045]

Ming GL. Turning by asymmetric actin. Nat Neurosci 2006;9:1201–1203. [PubMed: 17001333]

NIH-PA Author Manuscript

NIH-PA Author Manuscript

NIH-PA Author Manuscript

Ming GL, Song HJ, Berninger B, Holt CE, Tessier-Lavigne M, Poo MM. cAMP-dependent growth cone guidance by netrin-1. Neuron 1997;19:1225–1235. [PubMed: 9427246]

Ming GL, Wong ST, Henley J, Yuan XB, Song HJ, Spitzer NC, Poo MM. Adaptation in the chemotactic guidance of nerve growth cones. Nature 2002;417:411–418. [PubMed: 11986620]

Miniero R, Tardivo I, Curtoni ES, Segoloni GP, La Rocca E, Nino A, Todeschini P, Tregnaghi C, Rosati A, Zanelli P, Dall'Omo AM. Pregnancy after renal transplantation in Italian patients: focus on fetal outcome. J Nephrol 2002;15:626–632. [PubMed: 12495275]

Moon MS, Gomez TM. Adjacent pioneer commissural interneuron growth cones switch from contact avoidance to axon fasciculation after midline crossing. Dev Biol 2005;288:474–486. [PubMed: 16293241]

Muchmore, DC.; McIntosh, LP.; Russell, CB.; Anderson, DE.; Dahlquist, FW.; Norman, JO.; Thomas, LJ. Methods in Enzymology. Academic Press; 1989. Expression and nitrogen-15 labeling of proteins for proton and nitrogen-15 nuclear magnetic resonance; p. 44-73.

Mukhopadhyay G, Doherty P, Walsh FS, Crocker PR, Filbin MT. A novel role for myelin-associated glycoprotein as an inhibitor of axonal regeneration. Neuron 1994;13:757–767. [PubMed: 7522484]

Nilius B, Owsianik G, Voets T, Peters JA. Transient receptor potential cation channels in disease. Physiol Rev 2007;87:165–217. [PubMed: 17237345]

Perrin CL, Dwyer TJ. Application of two-dimensional NMR to kinetics of chemical exchange. Chemical Reviews 1990;90:935–967.

Phelps PE, Alijani A, Tran TS. Ventrally located commissural neurons express the GABAergic phenotype in developing rat spinal cord. J Comp Neurol 1999;409:285–298. [PubMed: 10379921]

Reimer U, Drewello M, Jakob M, Fischer G, Schutkowski M. Conformational state of a 25-mer peptide from the cyclophilin-binding loop of the HIV type 1 capsid protein. Biochem J 1997;326(Pt 1):181–185. [PubMed: 9337866]

Schiene-Fischer C, Yu C. Receptor accessory folding helper enzymes: the functional role of peptidyl prolyl cis/trans isomerases. FEBS Lett 2001;495:1–6. [PubMed: 11322937]

Serafini T, Colamarino SA, Leonardo ED, Wang H, Beddington R, Skarnes WC, Tessier-Lavigne M. Netrin-1 is required for commissural axon guidance in the developing vertebrate nervous system. Cell 1996;87:1001–1014. [PubMed: 8978605]

Shim S, Goh EL, Ge S, Sailor K, Yuan JP, Roderick HL, Bootman MD, Worley PF, Song H, Ming GL. XTRPC1-dependent chemotropic guidance of neuronal growth cones. Nat Neurosci 2005;8:730–735. [PubMed: 15880110]

Siekierka JJ, Hung SH, Poe M, Lin CS, Sigal NH. A cytosolic binding protein for the immunosuppressant FK506 has peptidyl-prolyl isomerase activity but is distinct from cyclophilin. Nature 1989;341:755–757. [PubMed: 2477714]

Sinkins WG, Goel M, Estacion M, Schilling WP. Association of immunophilins with mammalian TRPC channels. J Biol Chem 2004;279:34521–34529. [PubMed: 15199065]

Snyder SH, Lai MM, Burnett PE. Immunophilins in the nervous system. Neuron 1998;21:283–294. [PubMed: 9728910]

Song H, Ming G, He Z, Lehmann M, McKerracher L, Tessier-Lavigne M, Poo M. Conversion of neuronal growth cone responses from repulsion to attraction by cyclic nucleotides. Science 1998;281:1515–1518. [PubMed: 9727979]

Song H, Stevens CF, Gage FH. Astroglia induce neurogenesis from adult neural stem cells. Nature 2002;417:39–44. [PubMed: 11986659]

Song HJ, Poo MM. Signal transduction underlying growth cone guidance by diffusible factors. Curr Opin Neurobiol 1999;9:355–363. [PubMed: 10395576]

Steiner JP, Dawson TM, Fotuhi M, Glatt CE, Snowman AM, Cohen N, Snyder SH. High brain densities of the immunophilin FKBP colocalized with calcineurin. Nature 1992;358:584–587. [PubMed: 1380130]

Takahashi N, Hayano T, Suzuki M. Peptidyl-prolyl cis-trans isomerase is the cyclosporin A-binding protein cyclophilin. Nature 1989;337:473–475. [PubMed: 2644542]

Venkatachalam K, Montell C. TRP channels. Annu Rev Biochem 2007;76:387–417. [PubMed: 17579562]

NIH-PA Author Manuscript

NIH-PA Author Manuscript

NIH-PA Author Manuscript

Wang GX, Poo MM. Requirement of TRPC channels in netrin-1-induced chemotropic turning of nerve growth cones. Nature 2005;434:898–904. [PubMed: 15758951]

Xiao B, Tu JC, Petralia RS, Yuan JP, Doan A, Breder CD, Ruggiero A, Lanahan AA, Wenthold RJ, Worley PF. Homer regulates the association of group 1 metabotropic glutamate receptors with multivalent complexes of homer-related, synaptic proteins. Neuron 1998;21:707–716. [PubMed: 9808458]

Yuan JP, Kiselyov K, Shin DM, Chen J, Shcheynikov N, Kang SH, Dehoff MH, Schwarz MK, Seeburg PH, Muallem S, Worley PF. Homer binds TRPC family channels and is required for gating of TRPC1 by IP3 receptors. Cell 2003;114:777–789. [PubMed: 14505576]

Yuan JP, Zeng W, Huang GN, Worley PF, Muallem S. STIM1 heteromultimerizes TRPC channels to determine their function as store-operated channels. Nat Cell Biol 2007;9:636–645. [PubMed: 17486119]

Zeng W, Yuan JP, Kim MS, Choi YJ, Huang GN, Worley PF, Muallem S. STIM1 gates TRPC channels, but not Orai1, by electrostatic interaction. Mol Cell 2008;32:439–448. [PubMed: 18995841]

Zheng JQ. Turning of nerve growth cones induced by localized increases in intracellular calcium ions. Nature 2000;403:89–93. [PubMed: 10638759]

Zheng JQ, Felder M, Connor JA, Poo MM. Turning of nerve growth cones induced by neurotransmitters. Nature 1994;368:140–144. [PubMed: 8139655]

NIH-PA Author Manuscript
NIH-PA Author Manuscript
NIH-PA Author Manuscript

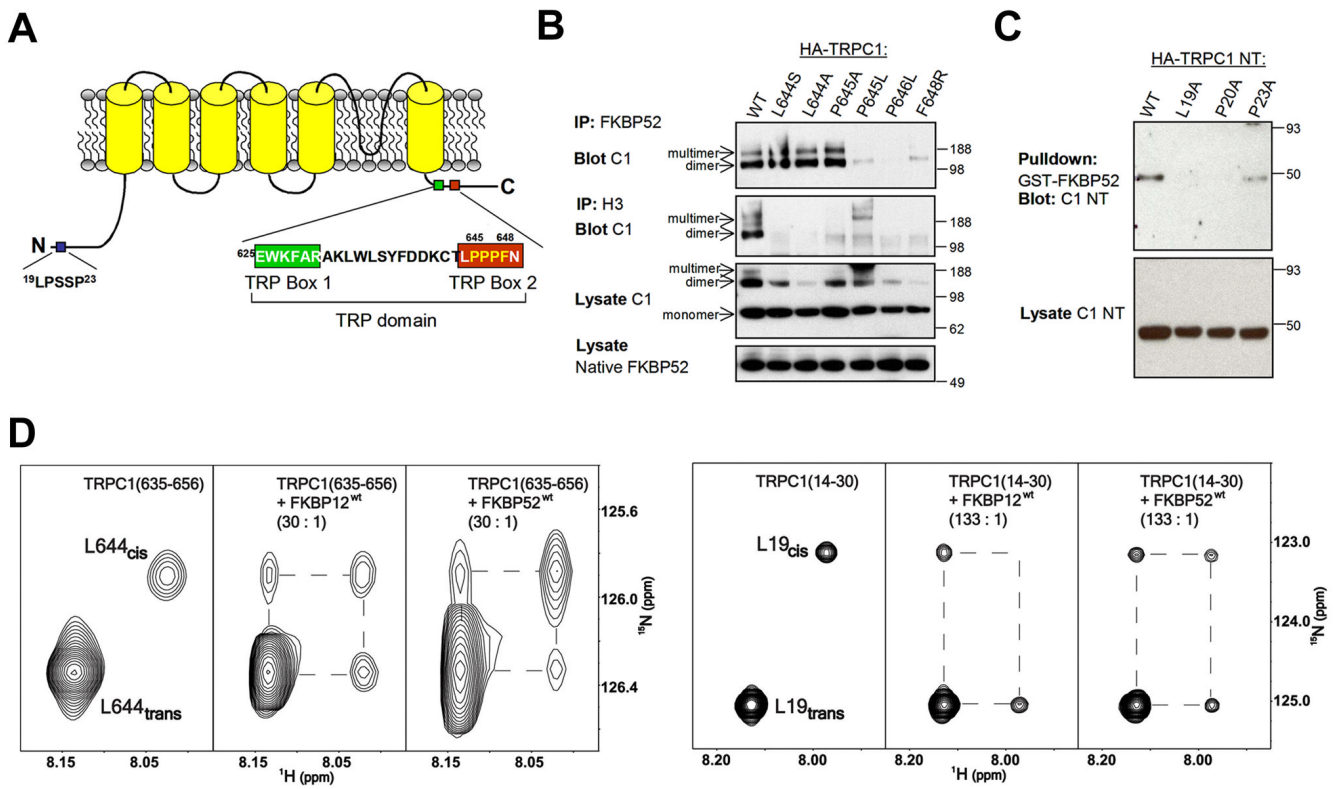

Figure 1. Binding and isomerization of TRPC1 by FKBP52 and FKBP12

(**A**) A schematic diagram of human TRPC1 indicating regions critical for FKBP52 (^{19}LPSSP^{23} and ^{644}LPPPF^{648}) and C-terminal Homer binding (^{645}PPPF^{648}).

(**B**) FKBP52 and Homer require similar, but not identical sequences of TRPC1 C-terminus for binding. Lysates of HEK293 cells expressing HA-TRPC1 constructs (C1) were assayed for co-IP with native FKBP52 or Homer 3 (H3).

(**C**) FKBP52 binds TRPC1 N-terminus (NT) and requires canonical Leu-Pro residues for binding. Lysates of HEK293 cells expressing HA-TRPC1 NT constructs were assayed for binding to GST-FKBP52.

(**D**) Catalysis of L19-P20 and L644-P645 peptidyl-prolyl bonds in TRPC1 mimic peptides by substoichiometric amounts of FKBP12 and FKBP52. Expansion of ^{1}H-^{15}N heteronuclear exchange spectra at 25°C showing amide signals of *cis* and *trans* isomers of L19 and L644 residues within TRPC1(14–30) and TRPC1(535–656) peptides, respectively. Conformational exchange between *cis* and *trans* isomers was slow on the NMR timescale ($k_{ex} < 0.1s^{-1}$) in absence of FKBPs resulting in distinct resonance signals for the two conformations (left). Upon addition of catalytic amounts of either FKBP12 or FKBP52 [30:1 TRPC1(635–656)/FKBP and 133:1 TRPC1(14–30)/FKBP] exchange peaks were observed connecting the *cis* and *trans* isomer resonances, denoted by dashed lines, indicating efficient acceleration of the isomerization rate by the enzymes.

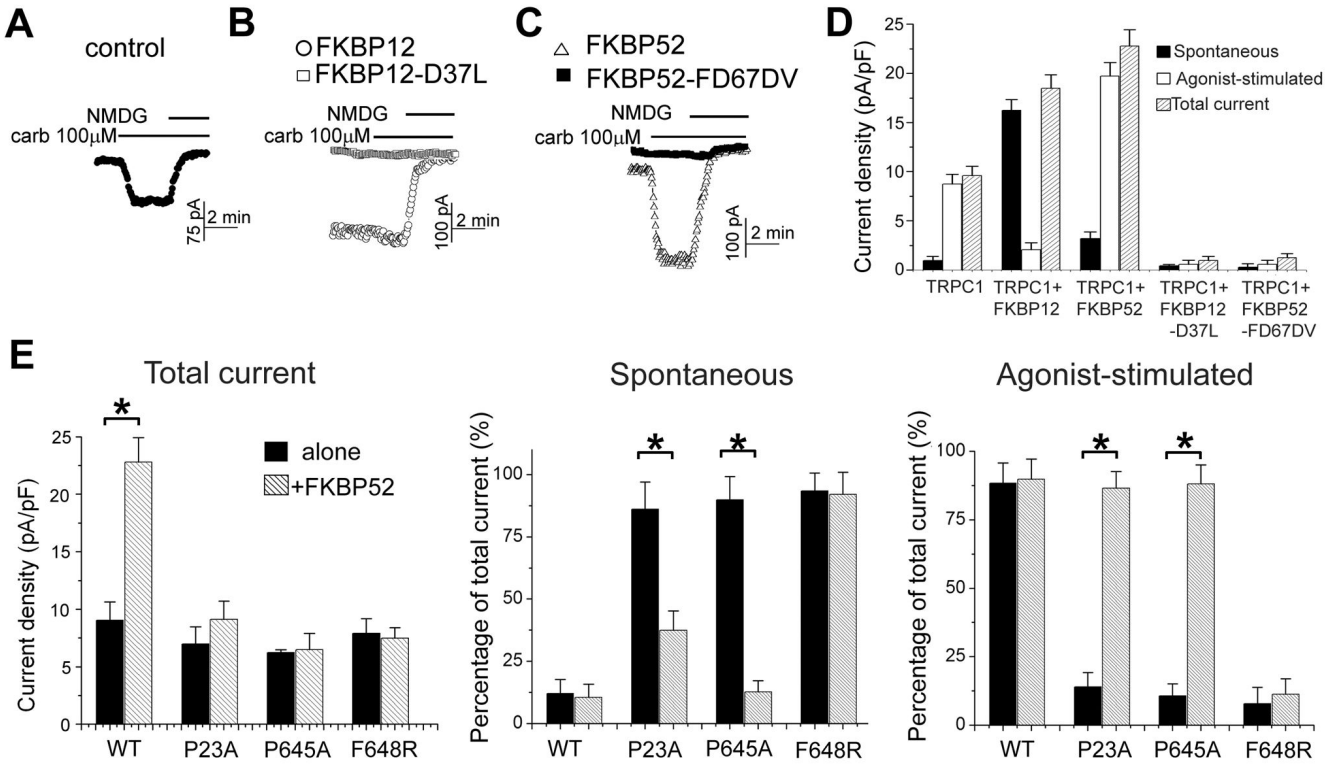

Figure 2. Differential roles of FKBP12 and FKBP52 in TRPC1 gating

(**A–C**) Sample traces of electrophysiology recordings of TRPC1 currents. HEK293 cells transfected with TRPC1 and empty vector (**A**), TRPC1 and FKBP12-WT (○) or FKBP12-D37L)(□)(**B**), TRPC1 and FKBP52-WT(△), or FKBP52-FD67DV(■)(**C**) were bathed in media containing 140 mM Na^+, then stimulated with 100 μM carbachol and finally incubated in Na^+-free media to determine the zero current.

(**D**) Summary of the spontaneous, receptor-activated and total current. Values represent mean ± SEM. (*: $p < 0.01$, Student t-test).

(**E**) Agonist-stimulated currents of select TRPC1 mutants were restored by co-expression of FKBP52. HEK293 cells were transfected with TRPC1-WT and the indicated TRPC1 mutants alone or together with FKBP52. Values represent mean ± SEM (n = 4–5) of the total, spontaneous and agonist-stimulated current (*: $p < 0.01$, Student t-test).

NIH-PA Author Manuscript NIH-PA Author Manuscript NIH-PA Author Manuscript

NIH-PA Author Manuscript
NIH-PA Author Manuscript
NIH-PA Author Manuscript

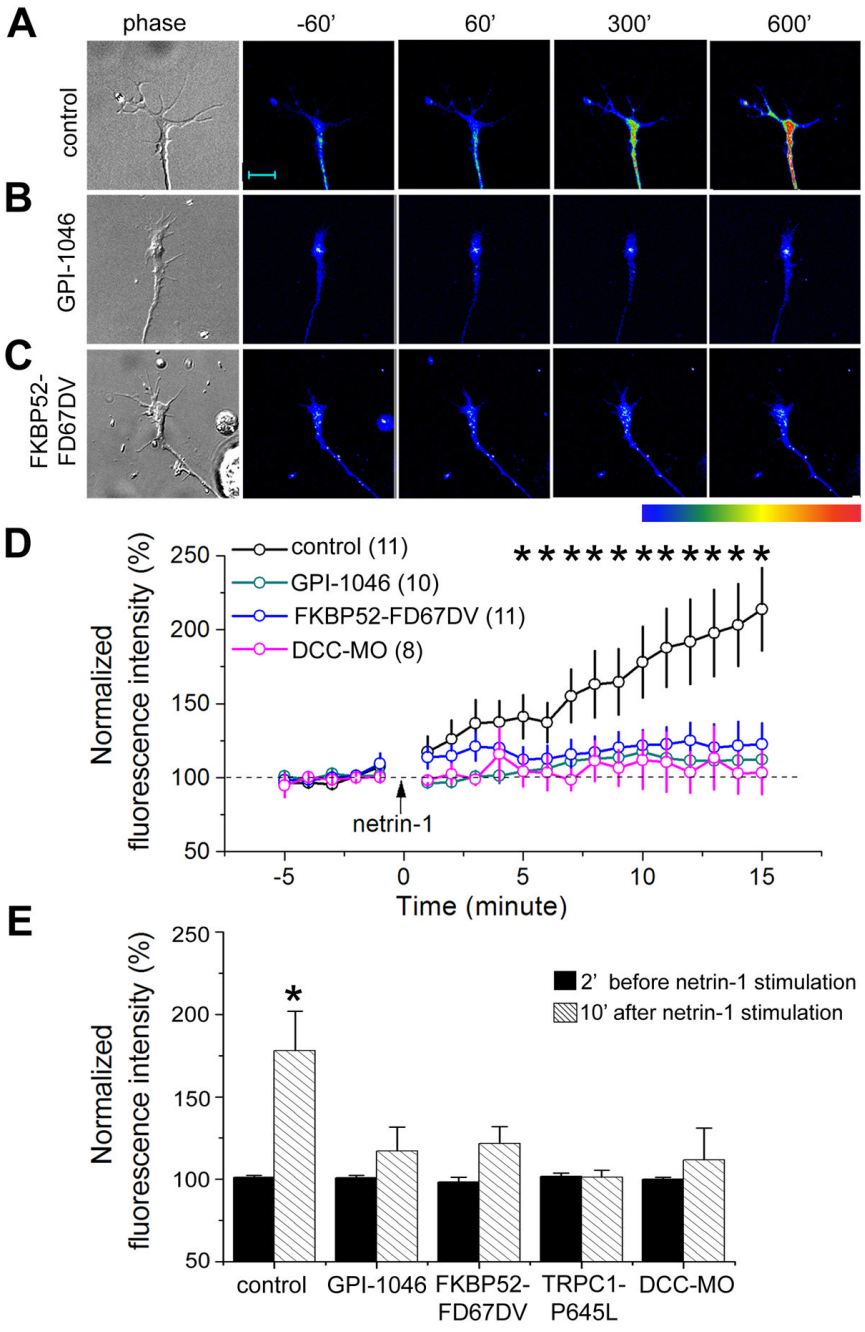

Figure 3. PPIase-dependent regulation of netrin-1-induced Ca^{2+} influx by FKBP52

(**A–C**) Bright-field and fluorescence images of growth cones of *Xenopus* spinal neurons loaded with Fluo-4 at different time points after stimulation with netrin-1 (10 ng/ml). Sample images show neurons from an un-injected embryo without (control, **A**) or with GPI-1046 (500 nM, **B**) in the bath, or from an FKBP52-FD67DV expressing neuron (**C**). Pseudocolor indicates Ca^{2+} levels with red as the highest and blue as the lowest. Scale bar: 10 μm.

(**D**) Time course of netrin-1-induced Ca^{2+} rise in growth cones under different conditions. The fluorescence intensity of each time point was normalized to the average fluorescence intensity of 5 mins baseline period before netrin-1 application for each neuron. Values represent mean ± SEM. (n = 8–11; *: $p < 0.01$, Bootstrap test).

NIH-PA Author Manuscript

NIH-PA Author Manuscript

NIH-PA Author Manuscript

(**E**) Summary of netrin-1-induced Ca^{2+} changes in growth cones. The fluorescence intensity was normalized to the average fluorescence intensity of 5 mins baseline levels prior to the netrin-1 application (5 ng/ml). Values represent mean ± SEM. (*: $p < 0.01$, Bootstrap test).

NIH-PA Author Manuscript
NIH-PA Author Manuscript
NIH-PA Author Manuscript

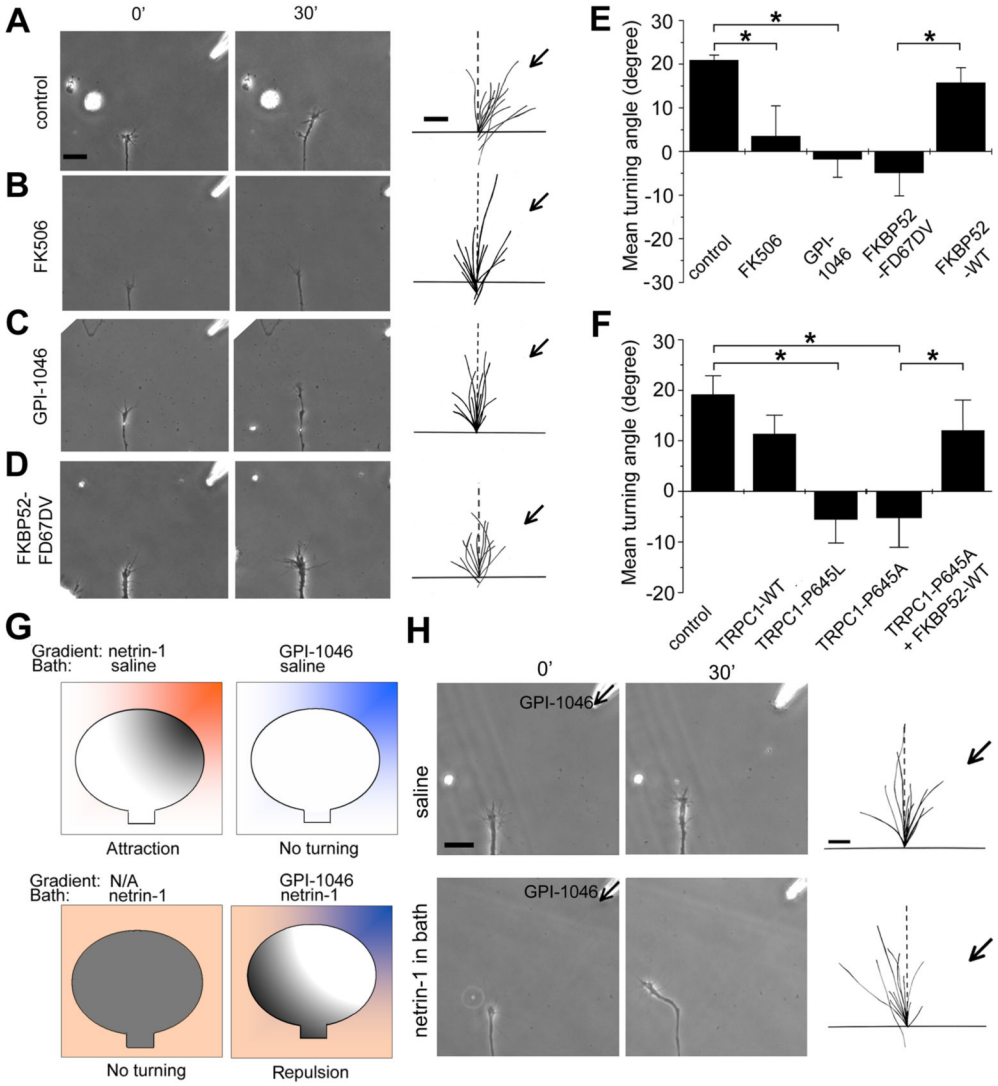

Figure 4. PPIase activity-dependent regulation of netrin-1 induced attractive growth cone turning responses of *Xenopus* spinal neurons by FKBP52

(**A–D**) Growth cone turning responses in a gradient of netrin-1 by neurons in the control medium (**A**), in the presence of bath application of FK506 (10 nM, **B**) or GPI-1046 (10 nM, **C**), and neurons derived from embryos injected with the mRNA encoding FKBP52-FD67DV (**D**), respectively. The left two columns of images show growth cones at the start (0′) and the end of exposure (30′) in a netrin-1 gradient (10 μg/ml in the pipette). Scale bar: 20 μm. The right column shows superimposed trajectories of neurite extension during the 30′ period for a sample population of 12 neurons under each condition. The origin is the center of the growth cone and the original direction of growth is vertical. Arrows indicate the direction of the gradient. Scale bar: 10 μm.

(**E**) The PPIase activity is required for netrin-1-induced growth cone attraction. Shown is the summary of turning angles under different conditions. Values represent mean ± SEM. (*: $p < 0.01$, Bootstrap test).

(**F**) FKBP52 regulates netrin-1-induced growth cone turning through its association with TRPC1. Values represent mean ± SEM. (*: $p < 0.01$, Bootstrap test).

(**G–H**) Netrin-1-induced PPIase activation is sufficient for attractive growth cone turning. Shown in (**G**) is a schematic illustration of experimental paradigms and models. Netrin-1 (orange); PPIase activity (gray); GPI-1046 (blue). Similar as in (**A–D**), shown in (**H**) are growth cone turning responses in a gradient of GPI-1046 (100 μM in the petite) in the normal medium, or with netrin-1 (10 ng/ml) in the bath.

NIH-PA Author Manuscript
NIH-PA Author Manuscript
NIH-PA Author Manuscript

NIH-PA Author Manuscript

NIH-PA Author Manuscript

NIH-PA Author Manuscript

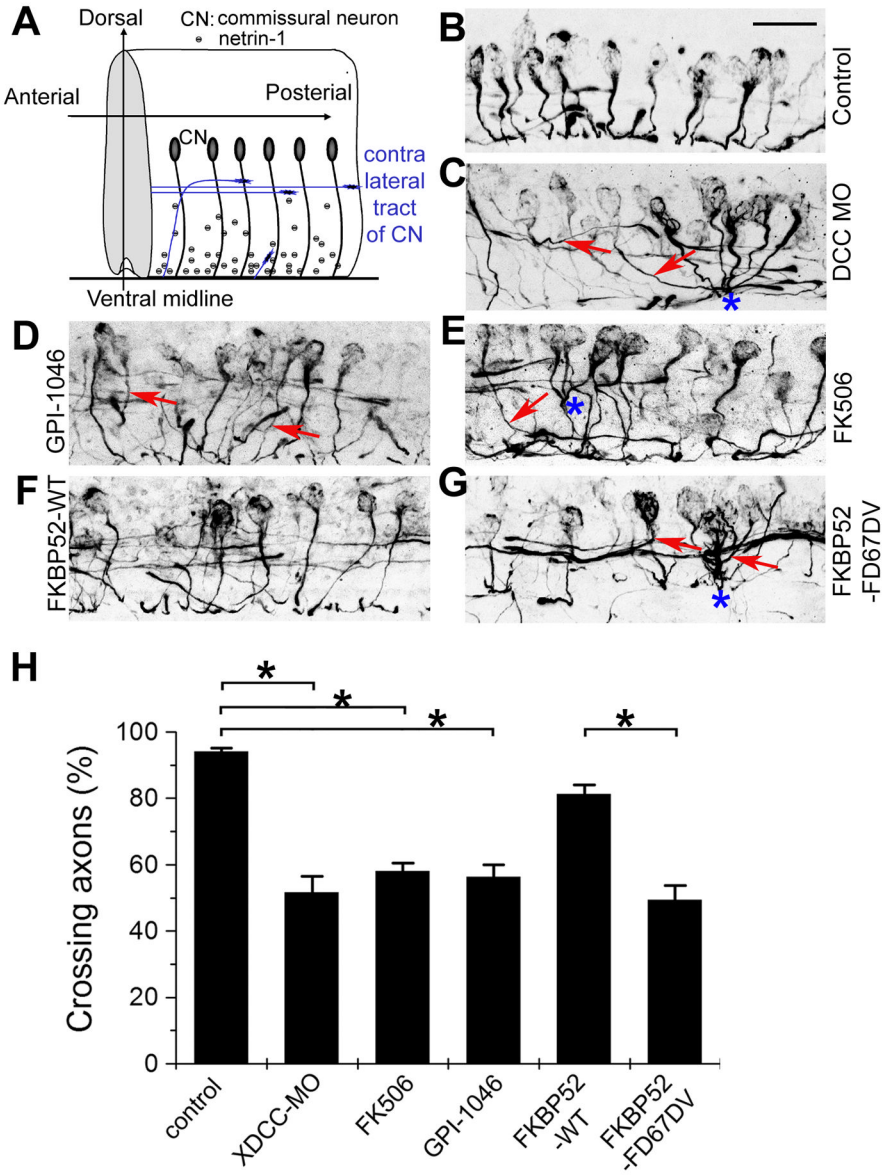

Figure 5. Requirement of PPIase activity of FKBP52 for midline axon guidance of commissural interneurons in the developing *Xenopus* spinal cord

(**A**) A schematic diagram of commissural interneuron projections in the developing embryonic *Xenopus* spinal cord.

(**B–G**) Sample images of the sagittal view of commissural interneurons and their axonal projections in the *Xenopus* spinal cord from stage 25 embryos. Shown are projections of Z-stack confocal images of 3A10 immunostaining of commissural interneuron axons from un-injected embryos (control, **B**), with treatment of GPI-1046 (0.5 μM, **D**) or FK506 (0.5 μM, **E**), or embryos injected with XDCC-MO (**C**), FKBP52-WT mRNA (**F**), FKBP52-FD67DV mRNA

(**G**), respectively. Arrows point to axons with defect in projection to the ventral middle line. Also note axons with premature fasciculation (highlighted with "*"). Scale bar: 40 μm.

(**H**) Quantification of the percentage of $3A10^+$ commissural interneurons with normal midline crossing under different experimental conditions. Values represent mean ± SEM. (n = 10–20 embryos; *: $p < 0.01$, Bootstrap test).

NIH-PA Author Manuscript
NIH-PA Author Manuscript
NIH-PA Author Manuscript

NIH-PA Author Manuscript
NIH-PA Author Manuscript
NIH-PA Author Manuscript

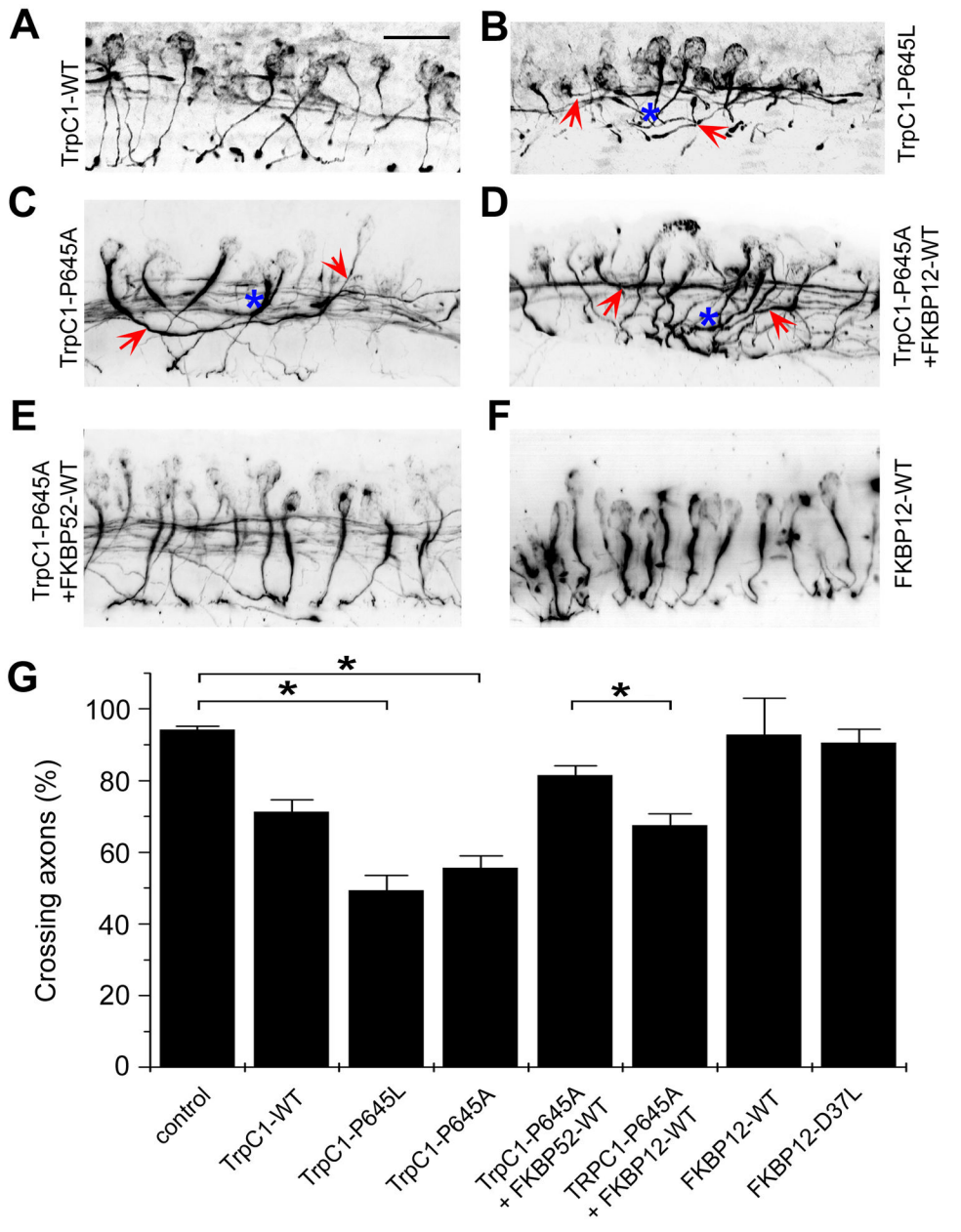

Figure 6. Requirement of association between TRPC1 and FKBP52, but not FKBP12, for midline axon guidance of commissural interneurons in the developing *Xenopus* spinal cord

(**A–F**) Sample images of the sagittal view of commissural interneurons and their axonal projections in the *Xenopus* spinal cord from stage 25 embryos. Shown are projections of Z-stack confocal images of 3A10 immunostaining of commissural interneuron axons from embryos injected with mRNAs encoding TRPC1-WT (**A**), TRPC1-P645L (**B**), TRPC1-P645A (**C**), TRPC1-P645A and FKBP12-WT (**D**), TRPC1-P645A and FKBP52-WT (**E**), and FKBP12-WT (**F**), respectively. Arrows point to axons with defect in projection to the ventral middle line. Also note axons with premature fasciculation (highlighted with "*"). Scale bar: 40 μm.

(**F**) Quantification of the percentage of $3A10^+$ commissural interneurons with normal midline crossing under different experimental conditions. Values represent mean ± SEM. (n = 10–20 embryos; *: $p < 0.01$, Bootstrap test).

NIH-PA Author Manuscript
NIH-PA Author Manuscript
NIH-PA Author Manuscript

NIH-PA Author Manuscript

NIH-PA Author Manuscript

NIH-PA Author Manuscript

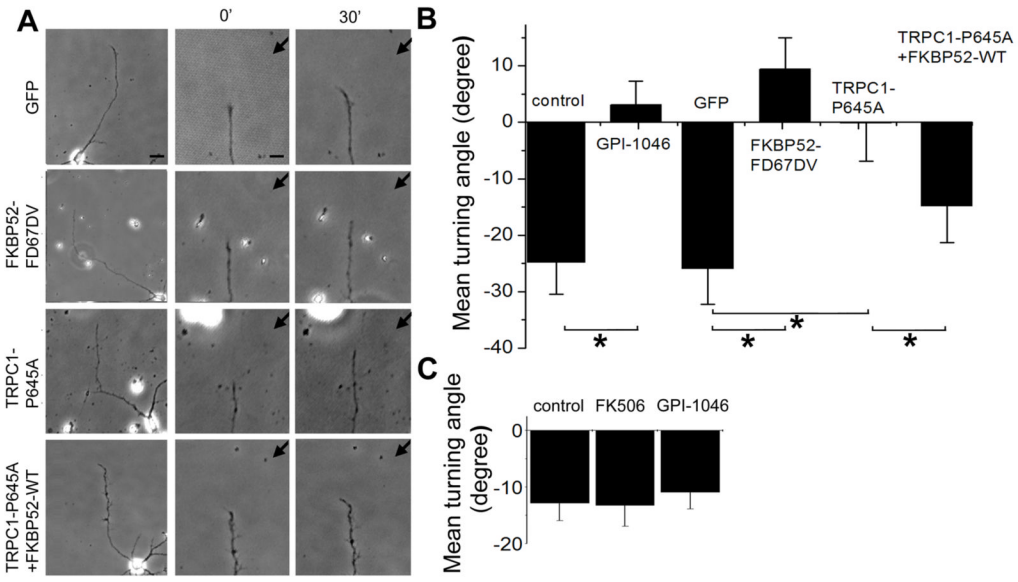

Figure 7. Requirement of PPIase activity of FKBP52 for MAG-, but not Sema3A-induced growth cone repulsion

(**A**) Axonal growth cone responses in a gradient of MAG (150 μg/ml in the pipette) of primary hippocampal neurons expressing GFP alone, or co-expressing GFP and FKBP52-FD67DV, TRPC1-P645A, TRPC1-P645A and FKBP52-WT, respectively. Images show growth cones at the start (0′; middle panel) and the end of exposure (30′; right panel) in a MAG gradient (150 μg/ml in the pipette). Also shown are images of the whole neuron at the end of the assay (left panel).

(**B**) Summary of growth cone turning angles of mammalian hippocampal neurons in response to a MAG gradient under different conditions. Values represent mean ± SEM (n = 13 to 32. *: $p < 0.01$, Bootstrap test).

(**C**) Lack of effects of PPIase inhibitors on Sema 3A-induced growth cone turning. Shown is a summary of growth cone turning angles of *Xenopus* spinal neurons in a gradient of Sema3A (50 μg/ml in the pipette) in the absence or presence of GPI-1046 (10 nM) or FK506 (10 nM) in the bath. Values represent mean ± SEM (n = 12 to 14). Note that no significant differences were found ($p < 0.05$, Bootstrap test).